Avoiding Local Minima for Deformable Curves in Image Analysis

Laurent D. Cohen

Abstract. We present an overview of part of our work over the past few years on snakes, balloons, and deformable models, with applications to image analysis. The main drawbacks of the active contour model being its initialization and minimization, we present three approaches that help to avoid being trapped in a local minimum of the energy. We introduced the balloon model to extract a contour being less demanding on the initial curve. In a more recent approach, based on minimal paths and geodesics, we find the global minimum of the energy between two points. A third approach is defined by a hybrid region-based energy taking into account homogeneity of the region inside the contour.

§1. Introduction

Active contour models, introduced by Kass, Witkin and Terzopoulos [15], and many variations on these deformable models have been studied for almost a decade and used for many applications. Using deformable models and templates, the extraction of a shape is obtained by giving an initial guess and through minimization of an energy composed of an internal regularization term and an external attraction potential (data fitting term), illustrated for example in [4,20,15,14,2,1]. Since the relevant shapes in medical images are usually smooth, the use of such models is particularly interesting for locating structures found in biomedical images and tracking their nonrigid deformation. We began using snakes for detecting the contour of Left Ventricular cavity of the heart in MR Images [10].

The main drawbacks of the active contour model being its initialization and minimization, we present three approaches that help to avoid being trapped in a local minimum of the energy, making initialization easier. We defined the balloon model [10,11] to extract the closed contour of an object being less demanding on the initial curve. This model was used as a first approach to make 3D reconstruction from cross sections [11]. A simplified 3D model was introduced as a stack of 2D balloons deforming simultaneously

Curves and Surfaces with Applications in CAGD
A. Le Méhauté, C. Rabut, and L. L. Schumaker (eds.), pp. 77–84.

ISBN 0-8265-1293-3.

[14]. To recover more general 3D surfaces in 3D medical images, the snake and balloon model was generalized to 3D and implemented with a finite element method in [14]. The normal inflation force appeared later as the basic evolution equation for many models with a moving front [5,18,25]. We also used recently a front evolution approach to find efficiently the global minimum of the snake energy [9]. A third approach making active contours less sensitive to initialization takes into account homogeneity of the region defined inside the curve. It combines edge and region terms, similar to Mumford-Shah energy [13]. Another way to make the algorithms more robust is to use parametric models like superquadrics or hyperquadrics. Once a global match with a rough shape is obtained, we have introduced ways to refine the shape given by the parametric model [8,3]. We also introduced a new mathematical formulation of some two-step iterative algorithms for deformable models, like deformable templates or B-spline snakes [17,2], using auxiliary variables [12].

§2. Active Contour Models or Snakes

We are looking for a plane curve $v(s) = (x(s), y(s))$ minimizing energy:

$$v \mapsto E(v) = \int_0^1 [w_1 \|v'(s)\|^2 + w_2 \|v''(s)\|^2 + P(v(s))] ds. \qquad (1)$$

This energy models mechanical properties that are between an elastic string (first order) and a more rigid rod or spline (second order). The minimization of the potential P attracts the curve to the interesting features in the image. In the original model [15], it is based on the gradient of image I : $P(v) = -\|\nabla I(v)\|^2$. In [11], we defined an attraction potential from a binary image of previously extracted edge points, using Gaussian convolution or a distance map potential. In the latter case, $P(v) = f(d(v))$ is a function of the Chamfer distance to edges. The attraction acts as a zero length string that links a point of the curve and a data point [14]. Related to robust statistics, f can be chosen bounded, in order to allow the string linked to the data to break [12]. We see in Figure 2 an example of distance map.

Starting from an initial estimate, we solve the evolution equation with fixed, free or periodic boundary conditions:

$$\frac{\partial v}{\partial t} - \frac{\partial}{\partial s}(w_1 \frac{\partial v}{\partial s}) + \frac{\partial^2}{\partial s^2}(w_2 \frac{\partial^2 v}{\partial s^2}) = F(v)$$

where $F = -\nabla P$ is the attraction force towards contours. This equation is equivalent to making a gradient descent of the energy converge to a minimum of (1).

In the 3D case [14], we model a surface that has physical properties between an elastic membrane (first order, like food wrapping plastic paper) and a thin plate (second order, for example projection transparencies).

The equations are solved using finite differences or finite elements. In any case, we can always write the iterative scheme in matrix form as

$$(Id + \tau A)V^t = (V^{t-1} + \tau F(V^{t-1})),$$

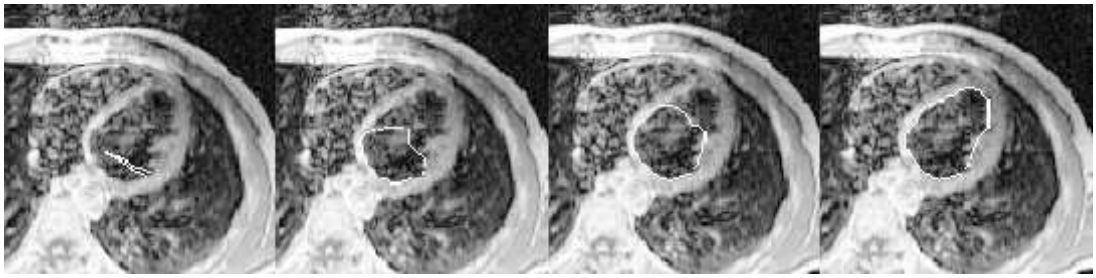

Fig. 1. MRI Image of the heart: Evolution of the balloon.

where V^t represents the vector of unknowns (nodes or degrees of freedom) of the discrete curve at iteration t.

§3. Balloon Model: Inflation Pressure Force

Usually, to make the curve converge to the right solution, the user has to provide an initial guess that is rather close to it. To make the curve converge to the solution, even when it is not close to it, we introduced the "Balloon model" [10]. We add a **pressure force** pushing outwards like inflating a "**balloon**". This gives the curve a more dynamic behavior

$$F_{balloon} = k\vec{n}(s), \tag{2}$$

where $\vec{n}(s)$ is the unit normal vector to the curve at point $v(s)$. The curve behaves like a balloon which is inflated. It is stopped by a strong edge but avoids the curve being "trapped" by spurious isolated edge points. This makes the result much less sensitive to the initial conditions. Since by inflating the model, the size of the curve increases, it may be necessary to increase the number of discretization nodes. This may be obtained by making reparametrization every few iterations, defining regularly spaced nodes.

We remark that this force derives from the inside area energy

$$E_{area} = -k \int_{insideregion} dA$$

that measures the area inside the region bounded by the curve. Minimization of such energy corresponds to get a region as large as possible. This is obtained by a pressure force in the outward normal direction.

We show an example of the balloon evolution in Figure 1. Starting from almost any curve inside the object permits the recovery of the whole boundary by inflating the curve like a balloon. This avoids the need for an initialization close to the solution.

Recently, much work has been done based on the evolution of a plane curve subject to a normal force. This was either in a purely mathematical framework or for various applications in image processing [21,22,5,18,6]. We

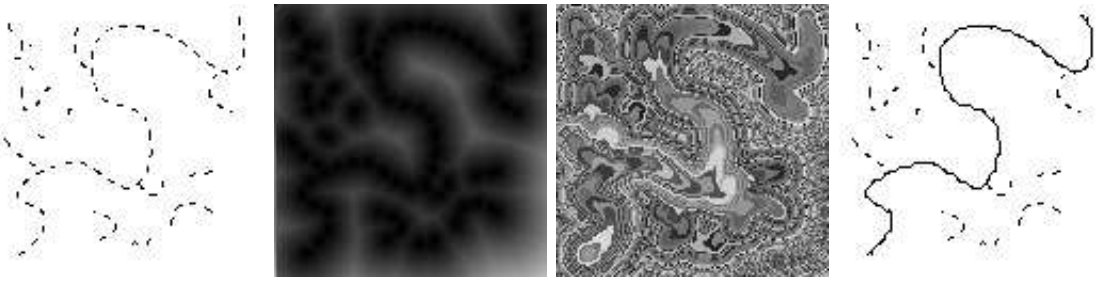

Fig. 2. Line image. From left to right: original, potential, minimal action (random look up table to show the level set propagation starting from the bottom left), minimal path between bottom left and top right.

also note the similarity between the evolution of a plane curve subject to a pressure force (2) and a dilatation in mathematical morphology.

The current trend to define a deformable curve or surface is to use an intrinsic geometric model [5,18]. The surface deforms as a front evolution in the normal direction of the zero level set of a 3D function. This function is "deformed" in order to make its zero level set follow the minimization of the potential. These are called either geometric or geodesic deformable models [6,7], implicit deformable surface [26], or bubbles [25]. This is an efficient way to change the topology. Other models also permit the curve or surface to change topology [24,19].

§4. Global Minimum using Geodesics

We now present an approach introduced in [9] which is based on normal front evolution of level sets to find the global minimum of the energy.

The minimization problem we are trying to solve is slightly different from (1). The reason we modified the energy is that we now have an expression where the internal regularization energy is included in the potential term. We can then solve the energy minimization in a way similar to that of finding the shortest path between two points on a surface using the method developed in [16]. The energy of the new model has the following form:

$$E(v) = \int_0^L [w\|v'(s)\|^2 + P(v(s))]ds = wL + \int_0^L P(v(s))ds = \int_0^L \tilde{P}(v(s))ds \quad (3)$$

where $\tilde{P} = P + w$. Here v is in the space of all curves connecting two given points (restricted by boundary conditions): $v(0) = p_0$ and $v(L) = p_1$, where L is the length of the curve. Contrary to the classical snake energy, here s represents the arc-length parameter, which means that $\|v'(s)\|^2 = 1$. This makes the energy depend only on the geometric curve $\mathcal{C}$ and not on the parameterization. The regularization term with w now exactly measures the length of the curve. To solve this minimization problem, we first search for the *surface of minimal action* U starting at $p_0 = v(0)$. At each point p of the

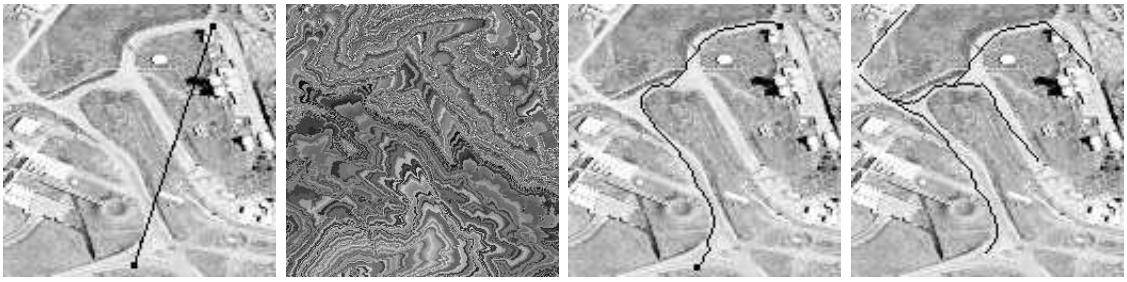

Fig. 3. Road Image. From left to right: initial data; minimal action level sets; path of minimal action connecting the two black points; many paths are obtained simultaneously connecting the start point on the upper left to 4 points.

image plane, the value of this surface U corresponds to the minimal energy integrated along a path starting at p_0 and ending at p:

$$U(p) = \inf_{v(L)=p} \left\{ \int_{\mathcal{C}} \tilde{P} ds \right\}. \tag{4}$$

Applying ideas of [16] to minimize our energy (3), it is possible to formulate a partial differential evolution equation describing the level set curves $\mathcal{L}$ of U:

$$\frac{\partial \mathcal{L}(s,t)}{\partial t} = \frac{1}{\tilde{P}} \vec{n}(s,t), \tag{5}$$

where $\tilde{P} = P + w$ and $\vec{n}(s,t)$ is the normal to the closed curve $\mathcal{L}(.,t) : S^1 \to \mathbb{R}^2$. This evolution equation is initialized by a curve $\mathcal{L}(s,0)$ which is a small circle surrounding the point p_0. It corresponds to a null energy. This evolution equation (5) is similar to a balloon evolution [11] with an inflation force depending on the potential.

This equation is solved using the Eulerian formulation for curve evolution introduced in [21] to overcome numerical difficulties and handle topological changes. Minimal action U can also be found efficiently using the fast marching method recently introduced by Sethian [23] as shown in [9].

The algorithm is thus composed of two steps. First, minimal action U from p_0 is computed using front propagation starting from an infinitesimal circle centered at p_0. Then a backpropagation is made, tracking the minimal path by gradient descent on U starting from p_1 ending at p_0. A synthetic example is presented in Figure 2. We demonstrate the performance of the proposed algorithm by applying it to an aerial road image in Figure 3. Since road areas are lighter and correspond to higher gray levels, we chose $P = -I$. Observe the way the level curves propagate faster along the path. We need only two points while with a classical snake, a very close initialization is necessary to avoid local minima (see [9]). Our approach can be used for the minimization of many paths emerging from the same point in one single calculation of the minimal action (Figure 3).

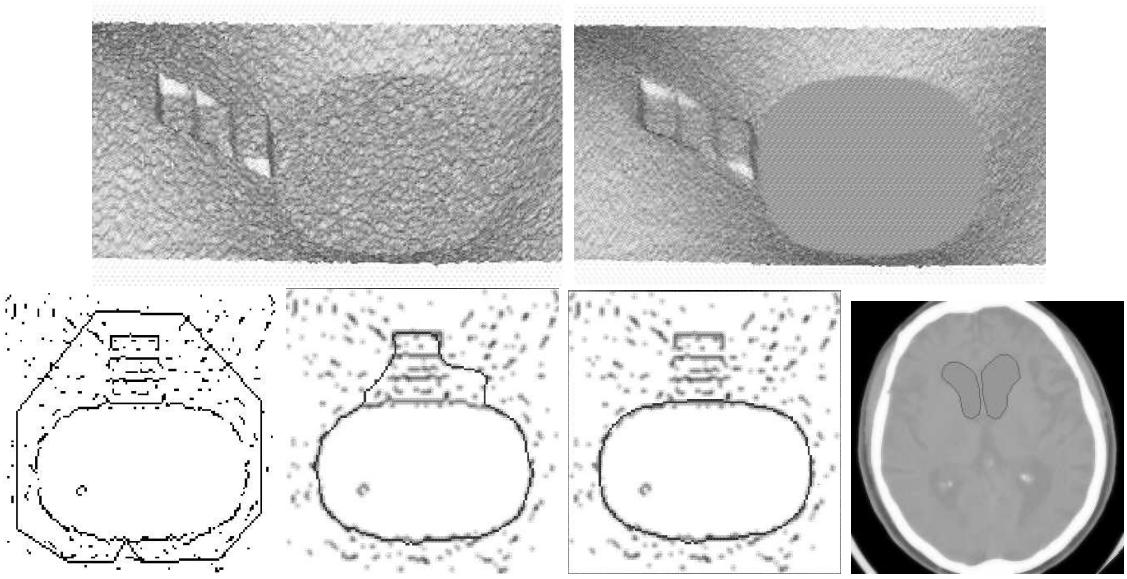

Fig. 4. Synthetic digital terrain model: above: original $z = I(x, y)$ and reconstruction $z = u(x, y)$ with our energy; below: On the left, initial curve is superimposed on an edge image obtained from I above. On the two middle images, we see the snake superimposed on the potential obtained from the edges. With the same initial curve on the left, a classic snake is stopped (middle-left) while the region term pushes the curve to the right boundary (middle-right). On the right, this is applied to two constant regions simultaneously to detect brain ventricles.

§5. Region-based Energy

Active contour models only take into account the information along the curve. This often stops the evolution of the curve, trapped in a local minimum. We take into account here the fact that the contour is the boundary of an homogeneous region by the introduction of a hybrid energy composed of region-based energy and boundary energy [13]. In [13] we used an active contour to detect a curve of discontinuities in a digital terrain model of a mountain and lake. The surface has to be smoothed and at the same time, we wish to recover the lake as a constant elevation region bounded by discontinuities.

We thus defined the reconstruction of a surface ($z = u(x, y)$) composed of two different kinds of regions. One has a constant elevation u_0 inside region L, the other is the background $(R - L)$. The boundary curve B between them is obtained with an active contour model v. This combines the two problems of surface reconstruction with discontinuities and contour detection. We minimize an energy that is function of the couple of unknowns (u, v):

$$E_g(u, v) = E_{snake}(v) + \int_L (u_0 - I(x, y))^2 dxdy + \int_{R-L} ((u - I)^2 + \lambda^2 \|\nabla u\|^2) \quad (6)$$

The algorithm successively minimizes energy E_g with respect to each of the two variables u and v. When u is given, minimization in v corresponds to

active contour evolution where new external forces are added that derive from the surface terms since L depends on v. This allows the model to take into account the fact that the level inside the region has to be homogeneous. This avoids the curve being trapped by spurious edges (see Figure 4). Initialization of the contour is made easier (see [13]). This property is not satisfied in classical active contours, where the curve "sees" only what happens locally along the curve and this may stop its evolution due to local minima.

Acknowledgments. Some of the presented work was done in collaboration with Nicholas Ayache, Eric Bardinet and Ron Kimmel. I would like to thank them, and express my wish that these fructuous collaborations go on.

References

1. Ayache, N., Medical computer vision, virtual reality and robotics, Image and Vision Computing, **13** (4) (1995), 295–313.
2. Ayache, N., P. Cinquin, I. Cohen, L. D. Cohen, F. Leitner, and O. Monga, Segmentation of complex 3D medical objects: a challenge and a requirement for computer assisted surgery planning and performing, in *Computer Integrated Surgery*. MIT Press, 1995, 59–74.
3. Bardinet, E., L. D. Cohen, and N. Ayache. Tracking medical 3D data with a deformable parametric model. in *Proc. ECCV'96*, U. K., I:317-328.
4. Blake, A. and A. Zisserman, *Visual Reconstruction*, MIT Press, 1987.
5. Caselles, V., F. Catté, T. Coll, and F. Dibos, A geometric model for active contours, Numer. Math. **66** (1993), 1–31.
6. Caselles, V., R. Kimmel, and G. Sapiro, Geodesic active contours, in *Proc. ICCV'95*, Cambridge, USA, June 1995, 694–699.
7. Caselles, V., R. Kimmel, G. Sapiro, and C. Sbert, 3D Object Modeling via Minimal Surfaces, in *Proc. ECCV'96*, Cambridge, U. K., 97-106.
8. Cohen, I., and L. D. Cohen. A hybrid hyperquadric model for 2-D and 3-D data fitting. in *Proc. 12th ICPR*, Jerusalem, 1994, B:403-405.
9. Cohen, L. D., and R. Kimmel. Global minimum for active contour models: A minimal path approach. in *Proc. CVPR'96*, San Francisco, June 1996.
10. Cohen, L. D., On active contour models. in *Active Perception and Robot Vision*. Springer, July 1989, 599–613.
11. Cohen, L. D., On active contour models and balloons, Computer Vision and Image Understanding **53**(2) (1991), 211–218.
12. Cohen, L. D., Auxiliary variables and two-step iterative algorithms in computer vision problems, in Journal of Mathematical Imaging and Vision **6**(1) (1996), 61–86. See also *Proc. IEEE ICCV'95*, Boston.
13. Cohen, L. D., E. Bardinet, and N. Ayache, Surface reconstruction using active contour models, in *Proc. Conference on Geometric Methods in Computer Vision*, San Diego, CA, SPIE **2031** (1993), 38–50.

14. Cohen, L. D., and I. Cohen, Finite element methods for active contour models and balloons for 2-D and 3-D images. in IEEE Trans. Pattern Anal. and Machine Intelligence **15**(11) (1993), 1131-1147.
15. Kass, M., A. Witkin, and D. Terzopoulos, Snakes: Active contour models, International Journal of Computer Vision, **1**(4) (1988), 321–331.
16. Kimmel, R., A. Amir, and A. Bruckstein, Finding shortest paths on surfaces, *Curves and Surfaces in Geometric Design*, P.-J. Laurent, A. Le Méhauté, and L. L. Schumaker (eds.), A. K. Peters, Wellesley MA, 1994, 259–268.
17. Leitner, F., I. Marque, S. Lavallée and P. Cinquin, Dynamic segmentation: finding the edge with snake-splines, in *Curves and Surfaces*, P.-J. Laurent, A. Le Méhauté, and L. L. Schumaker (eds.), Academic Press, New York, 1991, 1–4
18. Malladi, R., J. A. Sethian, and B. C. Vemuri, Shape modeling with front propagation: A level set approach. IEEE Trans. Pattern Anal. and Machine Intelligence **17**(2) (1995), 158–175.
19. McInerney, T. and D. Terzopoulos, Medical image segmentation using topologically adaptable snakes, in Springer, editor, *Proc. CVRMed'95*, Nice, France, April 1995, 92–101. See also ICCV'95, 840–845.
20. Mumford, D. and J. Shah, Boundary detection by minimizing functionals, in *Proc. CVPR'85*, San Francisco, June 1985, 22-26.
21. Osher, S. J. and J. A. Sethian. Fronts propagation with curvature dependent speed: Algorithms based on Hamilton-Jacobi formulations, J. Comput. Phys. **79** (1988), 12–49.
22. Sapiro G. and A. Tannenbaum, On invariant curve evolution and image analysis, Indiana Univ. Math. J. **42**(3) (1993), 985–1009.
23. Sethian, J. A., A fast marching level set method for monotonically advancing fronts, in Proc. Nat. Acad. Sci. **93**(4) (1996), 1591–1595.
24. Szeliski, R., D. Tonnessen, and D. Terzopoulos, Curvature and continuity control in particle-based surface models, in *Proc. Geometric Methods in Computer Vision*, San Diego, CA, SPIE **2031** (1993), 172-181.
25. Tek, H. and B. Kimia, Image segmentation by reaction-diffusion bubbles, in *Proc. ICCV'95*, Cambridge, USA, June 1995, 156–162.
26. Whitaker, R., Algorithms for implicit deformable models, in *Proceedings ICCV'95*, Cambridge, USA, June 1995, 822–827.

Laurent D. Cohen
CEREMADE, Université Paris IX Dauphine
Place du Maréchal de Lattre de Tassigny
75775 Paris cedex 16, France
Cohen@ceremade.dauphine.fr
http://www.ceremade.dauphine.fr/~cohen